Protein Science (1995), *4*:936–944. Cambridge University Press. Printed in the USA.

Investigation of a side-chain–side-chain hydrogen bond by mutagenesis, thermodynamics, and NMR spectroscopy

PHILIP K. HAMMEN,[1,4] J. MARTIN SCHOLTZ,[2] J. WILLIAM ANDERSON,[3] E. BRUCE WAYGOOD,[3] AND RACHEL E. KLEVIT[1]

[1] Department of Biochemistry, University of Washington, Seattle, Washington 98195
[2] Department of Medical Biochemistry and Genetics, Center for Macromolecular Design, Texas A&M University, College Station, Texas 77843
[3] Department of Biochemistry, University of Saskatchewan, Saskatoon, Saskatchewan S7N 5E5, Canada

(RECEIVED December 14, 1994; ACCEPTED February 24, 1995)

Abstract

Anomalous NMR behavior of the hydroxyl proton resonance for Ser 31 has been reported for histidine-containing protein (HPr) from two microorganisms: *Escherichia coli* and *Staphylococcus aureus*. The unusual slow exchange and chemical shift exhibited by the resonance led to the proposal that the hydroxyl group is involved in a strong hydrogen bond. To test this hypothesis and to characterize the importance of such an interaction, a mutant in which Ser 31 is replaced by an alanine was generated in HPr from *Escherichia coli*. The activity, stability, and structure of the mutant HPr were assessed using a reconstituted assay system, analysis of solvent denaturation curves, and NMR, respectively. Substitution of Ser 31 yields a fully functional protein that is only slightly less stable ($\Delta\Delta G^{folding} = 0.46 \pm 0.15$ kcal mol^{-1}) than the wild type. The NMR results confirm the identity of the hydrogen bond acceptor as Asp 69 and reveal that it exists as the *gauche*$^-$ conformer in wild-type HPr in solution but exhibits conformational averaging in the mutant protein. The side chain of Asp 69 interacts with two main-chain amide protons in addition to its interaction with the side chain of Ser 31 in the wild-type protein. These results indicate that removal of the serine has led to the loss of all three hydrogen bond interactions involving Asp 69, suggesting a cooperative network of interactions. A complete analysis of the thermodynamics was performed in which differences in side-chain hydrophobicity and conformational entropy between the two proteins are accounted for. This analysis, performed in the context of information afforded by the NMR studies, indicates that this network of interactions contributes ca. 4–5 kcal mol^{-1} to the conformational free energy of wild-type HPr.

Keywords: conformational free energy; hydrogen bond; NMR; protein stability; protein structure

The phosphocarrier protein, HPr, from the bacterial phosphoenolpyruvate:sugar phosphotransferase system is a small, soluble, monomeric, heat-stable protein that has been characterized in detail both by NMR and X-ray diffraction (for a review, see Herzberg & Klevit, 1994). Three-dimensional structures have been determined for HPrs from four different microorganisms: *Escherichia coli* (Klevit & Waygood, 1986; Hammen et al., 1991; van Nuland et al., 1992, 1994; Jia et al., 1993a), *Bacillus subtilis* (Herzberg et al., 1992; Wittekind et al., 1992), *Staphylococcus aureus* (Kalbitzer et al., 1991), and *Streptococcus faecalis* (Jia et al., 1993b). As expected for proteins that share a common function and 33–60% sequence identity, the folding topologies are very similar for all species studied. The distinguishing features are two or three α-helices on one face of a four-stranded antiparallel β-sheet, as shown in Figure 1 (Kinemage 1).

NMR studies performed in several laboratories on HPr from two microorganisms revealed an unusual resonance originating from a hydroxyl proton with a chemical shift other than that of bulk solvent. In these studies, the hydroxyl proton in *E. coli* had a chemical shift of ca. 5.75 ppm at pH 6.5, 30 °C (Hammen et al., 1991; van Nuland et al., 1994) and in *S. aureus* the chemical shift was 5.56 at pH 7.8, 35 °C (Kalbitzer et al., 1991). Gen-

Reprint requests to: Rachel E. Klevit, Department of Biochemistry, SJ-70, University of Washington, Seattle, Washington 98195; e-mail: klevit@u.washington.edu.

[4] Present address: Department of Biochemistry, Purdue University, West Lafayette, Indiana 47907.

Abbreviations: HPr, histidine-containing protein; *bs*HPr, *Bacillus subtilis* HPr; *ec*HPr, *Escherichia coli* HPr; wt-HPr, wild-type *ec*HPr; PTS, phosphoenolpyruvate:sugar phosphotransferase system; 2D, two-dimensional; NOESY, nuclear Overhauser enhancement spectroscopy; HMQC, heteronuclear multiple quantum correlation; TOCSY, total correlation spectroscopy; DQF-COSY, double quantum-filtered correlation spectroscopy.

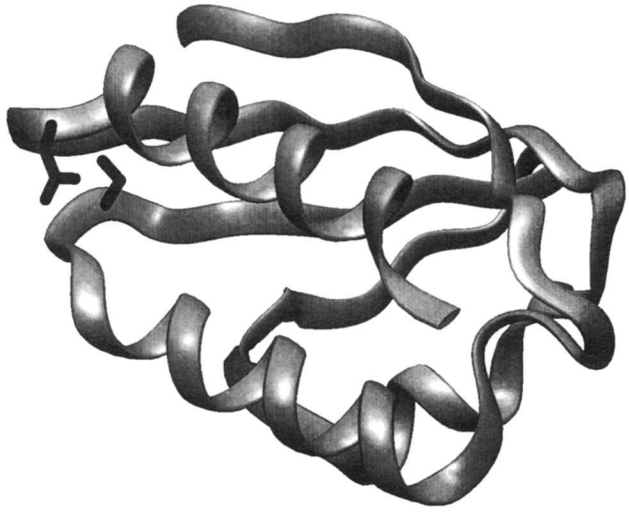

Fig. 1. Ribbon structure of *ec*HPr, showing the four-stranded β-sheet and the α-helices. Side-chain atoms for Ser 31 and Asp 69 are shown as black stick representations. The N-terminus is at the upper left-hand corner (coordinates from PDB file 1POH).

erally, hydroxyl protons exchange so rapidly with solvent protons that their resonances are only detected at the position of the H_2O resonance. The unusual resonances in the spectra of *E. coli* HPr and *S. aureus* HPr have both been assigned to the $O^{\gamma}H$ of Ser 31. Ser 31 is at the N-terminal end of one of the two internal strands in the β-sheet of HPr (see Fig. 1 and Kinemage 2). Our earlier report provided indirect evidence from NOE data that the hydroxyl proton in question interacts with some hydrogen bond acceptor in the turn that consists of Gly 67–Glu 68–Asp 69–Glu 70 at the C-terminal end of the adjacent β-strand. Crystallographic data on *ec*HPr are consistent with this interpretation, showing the O^{γ} of Ser 31 to be in proximity to one of the carboxylate oxygens of Asp 69 (Jia et al., 1993a).

A comparison of the amino acid sequences of all known HPrs reveals only a few absolutely conserved residues, one of which is Asp 69. Serine is found at position 31 in all known HPrs except HPr from *B. subtilis*, which contains alanine at this position. To investigate the role of the putative side-chain hydrogen bond involving Ser 31 in the structure and stability of *ec*HPr in solution, a mutant in which Ser 31 is substituted with alanine, S31A, was generated and characterized. The PTS activity, thermodynamic stability, and NMR properties of the mutant protein are reported here.

Results

Phosphotransfer activity of S31A

To test whether substitution of Ser 31 with alanine affected the function of *ec*HPr, phosphotransfer activity was measured using a reconstituted PTS. K_m and V_{max} values for enzyme I, enzyme II^{man}, enzyme II^{mtl}, and enzyme II^{nag} were measured and none was significantly different from those measured for the wild-type protein (Anderson et al., 1991). There was also no difference in the pH-dependent phosphohydrolysis rate of the phosphohistidine form of S31A at 37 °C.

Stability of wild-type and S31A HPr

The conformational stability of wild-type *ec*HPr and the S31A mutant was assessed by analysis of urea denaturation curves. The transitions were monitored spectroscopically by CD at 222 nm in 50 mM phosphate, pH 7.0, at 30 °C. Each transition was fully reversible and can be represented by a simple two-state folding reaction. Figure 2 shows the urea denaturation curves for the two proteins. Analysis of the urea denaturation data using the linear extrapolation method is shown as curves through the data. The details of the data analysis are described in the Materials and methods section. Because we find nearly identical *m*-values for the two proteins (see Fig. 2 legend), the difference in conformational stability of the proteins was calculated as:

$$\Delta\Delta G = \langle m \rangle \cdot \Delta C_{mid}, \quad (1)$$

where $\langle m \rangle$ is the average of the two *m*-values for the independent fits of the data (1,115 ± 20 cal mol^{-1} M^{-1}) and ΔC_{mid} is the difference in the midpoints of the unfolding transitions (0.41 ± 0.05 M urea; see Fig. 2 legend). This analysis yields a difference in conformational free energy ($\Delta\Delta G$) of 0.46 ± 0.15 kcal mol^{-1}, with wt-HPr being the more stable protein.

Characterization of the Ser 31 $O^{\gamma}H$ resonance

It is quite unusual to observe the OH resonance of a hydroxyl group in aqueous solution due to its rapid exchange with solvent protons. In order to characterize this resonance further, TOCSY spectra were collected for wt-HPr at increased temperatures. The Ser 31 $O^{\gamma}H$ resonance was still observed at 50 °C, the highest temperature at which 2D spectra could be collected due to a slow aggregation process that occurred at higher temperatures. Over the temperature range studied, most backbone amide resonances shifted upfield with temperature coefficients ranging from 0 ppb $°C^{-1}$ to −10 ppb $°C^{-1}$, with the majority of amides having coefficients ranging between −4 and −6 ppb $°C^{-1}$. The ^1H chemical shift of the Ser 31 $O^{\gamma}H$ changed in a similar

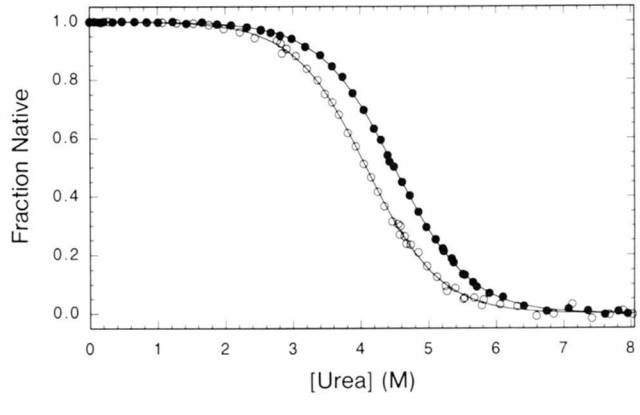

Fig. 2. Urea denaturation curves for HPr (closed circles) and S31A (open circles) as monitored by CD. Data have been normalized using the procedures described in the text. Analysis of the wild-type curve with the linear extrapolation method gives C_{mid} = 4.50 ± 0.02 M and an *m*-value of 1,100 ± 15 cal mol^{-1} (M urea)$^{-1}$, whereas the S31A curve gives C_{mid} = 4.09 ± 0.02 M and an *m*-value of 1,130 ± 15 cal mol^{-1} (M urea)$^{-1}$. Curves through the data represent the best-fit curves using these parameters. Details of the analysis are described in the text.

manner, with a temperature coefficient of -5 ppb $°C^{-1}$. The unusual persistence of this hydroxyl proton in the NMR spectrum and its temperature behavior are indicative of its being involved in a hydrogen bond and/or it being effectively shielded from contact with solvent.

NMR characterization of S31A HPr

In order to ascertain the structural consequences of substituting Ser 31, chemical shifts, J-coupling constants, NOEs, and NH exchange rates were measured and compared with values for wt-HPr. Resonance assignments for S31A were obtained from 2D homonuclear and heteronuclear spectra as described in the Materials and methods. Because the majority of resonances in the S31A spectra are not shifted relative to the wild-type spectrum, assigning the spectrum was straightforward.

Most backbone resonance chemical shifts for S31A are similar to those reported for wt-HPr, except near the site of mutation (residues 29–32) and in the turn at the end of the adjacent β-strand (residues 68–71) (Fig. 3; Kinemage 3). The largest ^1H and ^{15}N chemical shift changes observed are for residues Xxx 31, Asp 69, and Glu 70. The paucity of chemical shift perturbations other than at the site of mutation indicates that if any conformational changes have occurred due to the substitution of Ser 31 with alanine, they are small and local.

A comparison of backbone dihedral angles for the two proteins was performed using coupling constants measured in (^1H,^{15}N) HMQC-J spectra (Driscoll et al., 1990). These spectra provide a measure of $^3J_{NH\alpha}$, the magnitude of which varies as a function of ϕ. A residue-by-residue comparison between HPr and S31A revealed that the values of $^3J_{NH\alpha}$ for S31A are not detectably different from those previously reported for wt-HPr (Hammen et al., 1991). Due to substantial broadening of the NH resonances of Thr 30 and Ala 31, it was not possible to measure $^3J_{NH\alpha}$ for these residues in the mutant protein, limiting our ability to draw conclusions concerning the backbone structure at the site of mutation from this experiment. The results otherwise reveal that the mutation does not result in a change in backbone structure elsewhere in the protein.

Comparisons of NOESY spectra provide further evidence that the tertiary folds of HPr and S31A are similar. Throughout the NOESY spectra, cross peak patterns and relative intensities are similar, including those involving the mutated residue. Some differences were observed, but they involve low intensity peaks between methyl groups and/or aromatic protons, and therefore may arise from spin diffusion, making them difficult to interpret confidently in structural terms.

Information concerning side-chain conformations was obtained from (^1H,^{15}N) HNHB spectra, which yield information on the J-coupling between amide ^{15}N and the C^β proton(s) of each residue (Archer et al., 1991). The patterns of couplings observed are diagnostic for the preferred χ_1 rotamer populations normally seen in proteins. An intense cross peak identifies the β-proton that is in an anti-periplanar orientation with respect to the nitrogen atom. Observation of such a cross peak indicates that a residue exists predominantly in one of the *gauche* conformations, i.e., either *gauche*$^-$ ($\chi_1 = 60°$) or *gauche*$^+$ ($\chi_1 = 300°$). If a side chain exists predominantly as the *trans* conformer ($\chi_1 = 180°$), very weak or no HNHB cross peaks will be detected. If a side chain undergoes significant conformational averaging, HNHB peaks of approximately equal intensity may be observed for the two prochiral C^β protons or no peaks may be detected, depending on the degree and rate of conformational averaging.

Portions of HNHB spectra for wt-HPr and S31A are shown in Figure 4, with resonances for residues near the mutation site indicated. The observed cross peak patterns are very similar for most residues (see, for example, Phe 29 and Glu 70). In contrast, the HNHB pattern observed for Asp 69 differs in the two spectra. In wt-HPr, an intense cross peak is observed at the chemical shift of the downfield β-proton (3.35 ppm), indicating that Asp 69 exists predominantly in one of the *gauche* side-chain conformations. Strong NOEs are observed between the H^α and both of the β-protons in Asp 69. Together, the information from HNHB and NOESY spectra indicate that Asp 69 exists as the *gauche*$^-$ conformer in wt-HPr. In the HNHB spectrum of S31A, cross peaks for Asp 69 are very weak, indicating that the side chain is either predominantly in the *trans* conformation or that it is conformationally averaged. In NOESY spectra of S31A, cross peaks are observed between the NH and both $C^\beta H$ and between the $C^\alpha H$ and both $C^\beta H$ resonances of Asp 69. These NOE observations are not consistent with a single rotamer conformation having $\chi_1 = 180°$. Therefore, the data are most consistent with a conformationally averaged side chain for Asp 69 in S31A.

A possible outcome of the loss of the hydrogen bond donor Ser 31 is the formation of a new hydrogen bond involving the hydrogen bond acceptor. To probe potential differences in backbone hydrogen bonds in S31A, amide exchange rates were measured and compared with those in wt-HPr. Exchange rates were assessed in three different ways. In some cases, increased exchange rates with solvent are manifested in NH resonance broadening that is severe enough to be observed directly. Significant broadening was observed for the amide protons of Thr 30 and Ala 31 in S31A, suggesting that these protons are very accessible to solvent in the mutant. Exchange rates of slowly exchanging amide protons (exchange rate constants <0.1 min^{-1}) were measured by following the change in NH cross peak volume as protons exchanged for deuterons from the solvent in a sample of protein dissolved in D_2O (see the Materials and methods). Exchange rate constants measured from these experiments performed on wild-type and S31A HPr were not significantly different. In addition, no new slowly exchanging amide protons were observed for S31A. The exchange behavior of fast-exchanging amide protons (exchange rate constants >0.1 min^{-1}) was probed using relative cross peak intensities in HMQC spectra acquired with and without water saturation (Spera et al., 1991). Only one amide showed significantly different behavior in the two proteins. In wt-HPr, the NH of E68 exchanges with a rate constant of 2.0 s^{-1} at pH 6.5, 7.2, and 8.1. A pH-independent rate constant is characteristic of exchange behavior that is due largely to magnetization transfer. In S31A, the NH of E68 exchanges with a rate constant of 8.2 s^{-1} at pH 6.5 and $\sim$20 s^{-1} at the higher pH values. This behavior indicates that chemical exchange is involved and that this amide proton is more accessible to solvent in S31A than in wt-HPr.

Discussion

The observation of a shifted, slowly exchanging $O^\gamma H$ resonance for Ser 31 led us to posit that this side chain is involved in a strong hydrogen bond in wt-HPr (Hammen et al., 1991).

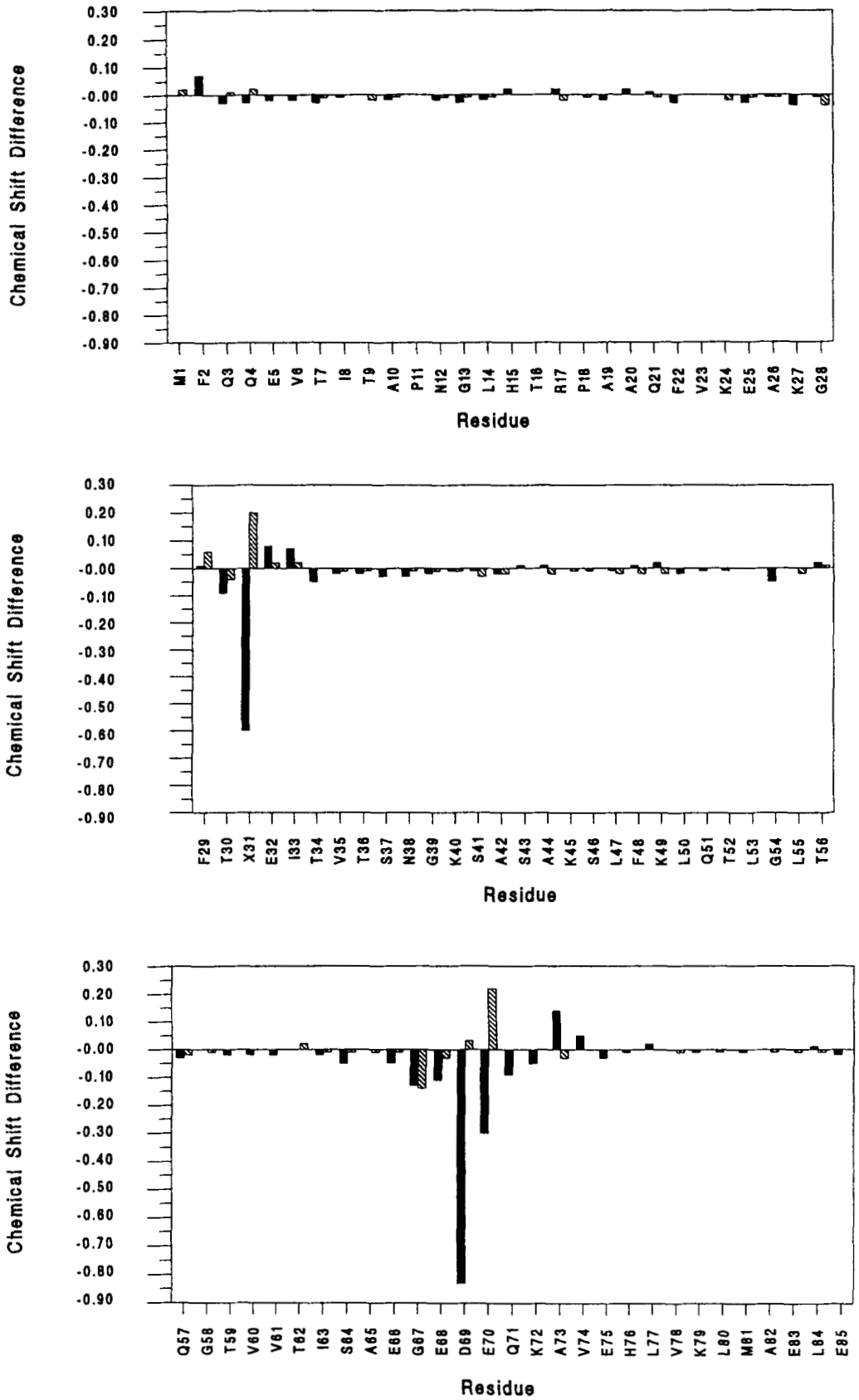

Fig. 3. Chemical shift differences for backbone proton resonances. Dark bars indicate NH chemical shifts and light bars indicate $C^{\alpha}H$ chemical shifts. Values represent the difference ($\delta_{wt\text{-}HPr} - \delta_{S31A}$) in ppm. A positive value indicates that the chemical shift of a resonance in S31A is upfield relative to its chemical shift in wt-HPr.

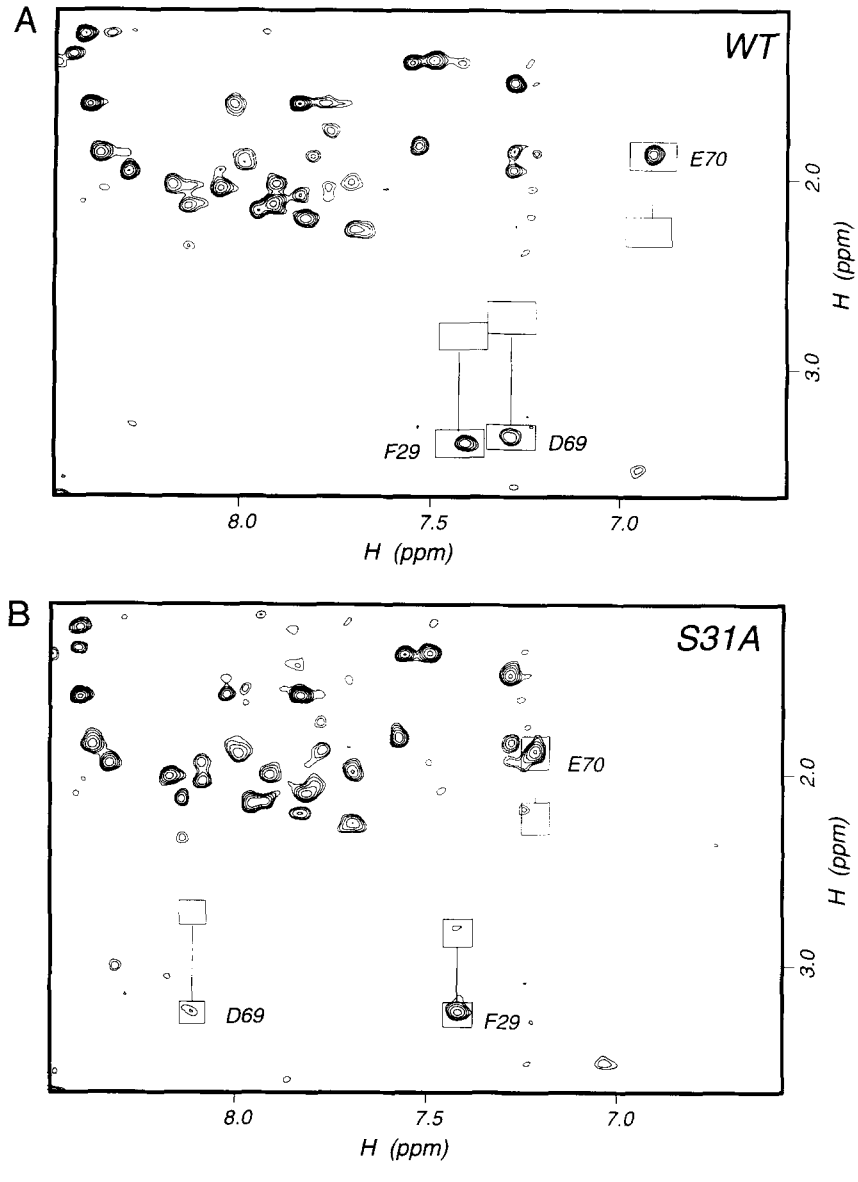

Fig. 4. Portions of HNHB spectra for wt-HPr (**A**) and S31A (**B**). Boxes indicate the resonance positions of the two prochiral C^{β} protons for residues Phe 29, Asp 69, Glu 70.

To test this hypothesis and to further characterize the importance of such an interaction to the structure, function, and stability of HPr, we designed and generated a mutant in which the serine is replaced by an alanine. The results reported here show that this substitution results in a fully active HPr molecule. Consistent with its activity, NMR parameters such as chemical shifts, $^3J_{NH\alpha}$, and NOEs indicate that the substitution does not result in any global conformational changes. Likewise, the far-UV CD spectra of the two proteins are identical, suggesting that no gross conformational change has occurred upon mutation (data not shown). Indeed, the only structural difference detected by NMR studies on S31A involves the side chain of Asp 69. In solution, Asp 69 exists predominantly as the *gauche*$^-$ rotamer in wt-HPr, whereas the side chain is conformationally averaged in S31A. Thus, the loss of hydrogen bond donor at position 31 affects the dynamics of Asp 69, the putative hydrogen bond acceptor. These results offer strong support for the hypothesis that the side chains of Ser 31 and Asp 69 are indeed involved in a hydrogen bond in solution. This conclusion verifies the interpretation of the structures determined crystallographically (Jia et al., 1993a) and in solution (van Nuland et al., 1994). Each of these structures suggested, on the basis of observed proximity, that the hydrogen bond acceptor for Ser 31 could be an O^{δ} of Asp 69 (see Fig. 5). The hydrogen bond predicted in the crystal structure (PDB file 1POH) has the following geometric parameters: donor-acceptor distance, 2.7 Å and donor-hydrogen-acceptor angle, 175°.

Urea denaturation studies reveal that S31A is slightly less stable than wt-HPr, with a difference in conformational free energy of 0.46 ± 0.15 kcal mol^{-1} for the two proteins. This value reflects all factors that contribute to the proteins' stability, not just the loss of a hydrogen bond. In their analysis of hydrogen bonding in RNase T1, Shirley and colleagues proposed a procedure to estimate the contribution to $\Delta\Delta G^{folding}$ due to the difference in hydrophobicity, which involves $\Delta G^{transfer}$ (Fauchère & Pliska, 1983) normalized by the degree of accessibility of the side chain

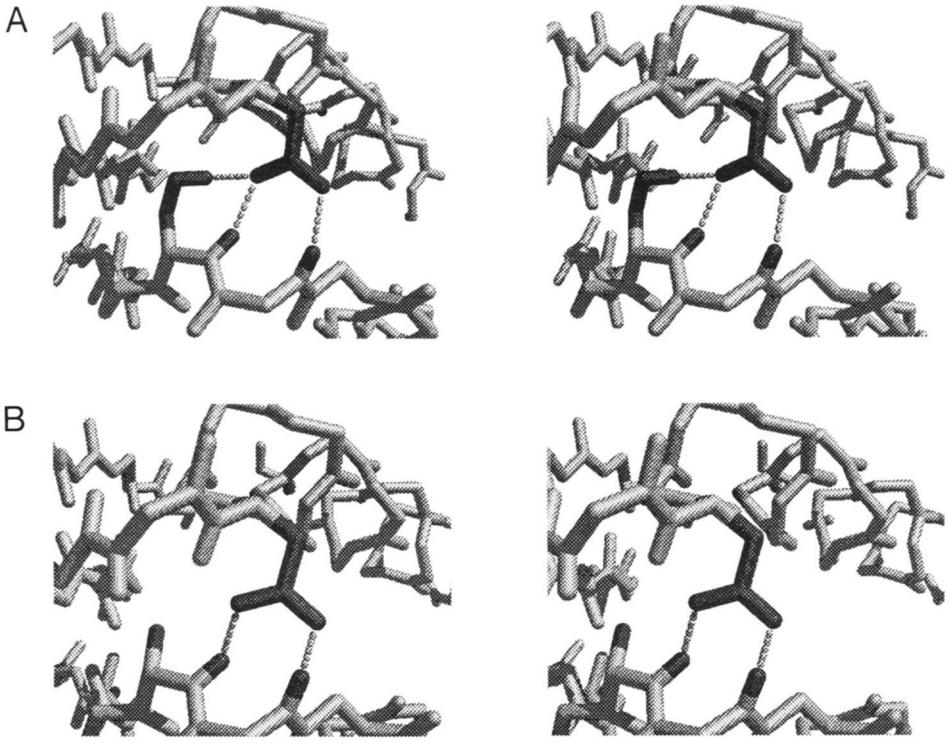

Fig. 5. Stereo views of the structures of HPr in the region around residues 31 and 69. **A:** *ec*HPr (PDB file 1POH). **B:** *bs*HPr (PDB file 2HPR). Main chain is depicted in light gray. Side chains of residues 31 and 69 and amide protons of residues 30 and 31 are depicted in dark gray. Dotted lines represent potential hydrogen bond interactions involving the carboxylate oxygens of Asp 69.

that was mutated (Shirley et al., 1992). The side chain of Ser 31 is completely buried in the crystal structure of wt-HPr and therefore its substitution with alanine would be expected to increase the stability of the mutant by ca. 0.4 kcal mol^{-1}. Using this value to correct the measured $\Delta\Delta G^{\text{folding}}$ yields ca. 0.9 kcal mol^{-1} of conformational free energy. If no other differences exist between the wt-HPr and the mutant protein, as was assumed to be the case in the analysis of Ser to Ala mutants of RNase T1, this value would correspond directly to the free energy associated with the hydrogen bond that was lost due to the mutation. We note that the value of 0.9 kcal mol^{-1} agrees well with the average value of 0.8 kcal mol^{-1} obtained for hydrogen bonds involving serine side chains, based on three different Ser to Ala mutants of RNase T1 (Shirley et al., 1992).

As pointed out by Shirley and colleagues, there are three possible fates for the hydrogen bond acceptor: (1) it could form a new hydrogen bond in the mutant protein; (2) it could form a hydrogen bond with solvent; or (3) it could fail to form any hydrogen bonds in the mutant. Because of the nature of the measurements made, analysis of the RNase T1 data was performed under the assumption that the hydrogen bond acceptor did not contribute significantly to the difference in free energy measured. In the studies presented here on HPr, we have additional information from NMR results that allows us to distinguish among these possibilities. In particular, we know that the side chain of Asp 69 is fixed and buried in wt-HPr and is conformationally averaged in S31A. These properties will certainly have an effect on conformational free energy and must be accounted for in a complete analysis of the free energy associated directly with hydrogen bonding.

The difference in mobility observed for the side chain of Asp 69 will contribute to a difference in conformational entropy between the two molecules. Pickett and Sternberg (1993) proposed an empirical scale for side-chain conformational entropy based on distributions of rotamers observed in high-resolution crystal structures. Their estimate for the entropic cost ($T\Delta S$ at 303 K) for fixing an aspartic acid would be 1.26 kcal mol^{-1}, which will favor the mutant in this case. An additional contribution to conformational entropy will be the difference between the fixed serine side chain in wt-HPr and an alanine in S31A. Because there is no entropic contribution from an alanine side chain, the mutant will be favored by the entropic cost associated with fixing the serine side chain, estimated to be 1.73 kcal mol^{-1}. Thus, the total entropic difference between S31A and wt-HPr is estimated to be the sum of the values for fixing Asp 69 and Ser 31, 2.99 kcal mol^{-1}, favoring S31A.

The conformational averaging of Asp 69 in S31A indicates an additional correction that should be made in the analysis, namely the cost of burying that side chain in wt-HPr. An accurate assessment of this contribution requires knowledge of the accessibility of the side chain in the mutant, which NMR results do not yield directly. Analysis of the crystal structure of wt-HPr reveals that the side chain of Asp 69 can be rotated from its *gauche*$^-$ conformation all the way around to a *gauche*$^+$ position, passing through the *trans* conformation, without steric clashes (see the Materials and methods). Within this range of side-chain conformations, Asp 69 goes from a buried environment to a completely solvent-accessible one. The estimated conformational free energy associated with burying an aspartic acid ranges from 0.08 to 1.05 kcal mol^{-1}, depending on the scale used (Sharp et al., 1991; Fauchère & Pliska, 1983, respectively). Because we cannot say whether Asp 69 is completely solvent accessible in S31A, these values would represent an upper limit for the contribution.

Adding all contributions to the measured $\Delta\Delta G^{\text{folding}}$ yields 3.8 or 4.9 kcal mol^{-1}, depending on the hydrophobicity scale

used for the aspartic acid. (If Asp 69 remains buried but conformationally averaged in S31A, a formal possibility that we believe to be unlikely, a value of 3.9 kcal mol^{-1} is obtained.) This value should represent the difference in free energy between the two proteins attributable to hydrogen bonding. Although we designed the mutant S31A with the intention of removing a single hydrogen bond, the NMR results show that more than just the Ser 31–Asp 69 side-chain–side-chain hydrogen bond has been lost in the mutant protein. As shown in Figure 5, the crystal structure of wt-HPr predicts that the side-chain carboxylate oxygens may serve as hydrogen bond acceptors to two main-chain amides, from residues 30 and 31, in addition to the hydrogen bond to the serine hydroxyl. The increased amide exchange rates observed for the resonances of Thr 30 and Ser 31 in S31A in addition to the conformational averaging exhibited by Asp 69 clearly indicate that these two main-chain hydrogen bonds have also been lost in S31A. Thus, the 3.8–4.9 kcal mol^{-1} corresponds to the free energy of all three hydrogen bonds. If each interaction contributes equally, an average value of 1.3–1.6 kcal mol^{-1} per hydrogen bond would be obtained; a range that agrees with the estimates of hydrogen bond strengths found in biomolecules and model compounds (see Shirley et al., 1992, for a complete discussion). We believe, however, that the Ser 31–Asp 69 side-chain–side-chain hydrogen bond may contribute more than the other two interactions because its removal results in the loss of all three hydrogen bonds, indicating that the two main-chain interactions (Asp 69 to the main-chain NH of Thr 30 and Ser 31) do not contribute enough free energy to overcome the entropic cost of fixing and burying the aspartic acid. It is perhaps more accurate to view these interactions as a cooperative network, because the removal of one of the interactions abrogates the others. In this case, it is difficult to assign specific contributions to each of the individual hydrogen bonds.

Because *bs*HPr has the same pair of residues at positions 31 and 69 as S31A, it is interesting to compare the behavior of these residues in this wild-type protein. Intriguingly, the side chain of Asp 69 in *bs*HPr is not conformationally flexible, but exists in the same rotamer conformation as in wt-*ec*HPr in solution (P. Rajagopal & R. Klevit, unpubl. obs.) as well as in the crystal structure (PDB file 1POH). The position of Asp 69 in *bs*HPr and the hydrogen bond interactions predicted for its side-chain oxygens are illustrated in Figure 5. In the crystal structure of *bs*HPr, there are potential interactions involving the carboxylate oxygens of Asp 69 and the backbone amide groups of Asp 30 and Ala 31. In contrast to S31A, however, the NMR properties of the Asp 69 side chain and of the two main-chain amide protons are consistent with these interactions being present in *bs*HPr solution. We note that the carboxylate oxygen to main-chain amide distances are shorter for Asp 69 in the *bs*HPr structure than in the wt-*ec*HPr structure (carboxylate oxygen to amide nitrogen distances of 2.64 Å, 2.74 Å in *bs*HPr and 2.99 Å, 3.02 Å in *ec*HPr). Thus, in the case of *bs*HPr, these two hydrogen bonding interactions may contribute enough free energy to overcome the entropic cost of fixing and burying Asp 69.

This study was initiated by the observation of the unusual NMR behavior of the hydroxyl proton of Ser 31. A combination of thermodynamic and solution NMR measurements has allowed us to perform a detailed analysis of a hydrogen bonding interaction in a protein. The results indicate that a cooperative network of hydrogen bonding interactions involving the side chains of Asp 69 and Ser 31 and two main-chain amide groups contribute a significant amount, ca. 4–5 kcal mol^{-1}, to the conformational free energy of wt-HPr. We conclude that the behavior of the Ser 31 proton is due to its involvement in this stable network of interactions and to its solvent-inaccessible environment. Although several other reports of slowly exchanging hydroxyl proton resonances have been reported in solution NMR studies (e.g., Driscoll et al., 1987; Feng et al., 1989; Gao et al., 1990), to our knowledge this is the first NMR-based study aimed at characterizing such a resonance in detail. As illustrated here, the combination of mutagenesis, thermodynamics, and NMR studies represents a powerful approach to dissecting specific interactions and their contributions to protein conformational free energy. Similar studies in other systems amenable to such techniques will undoubtedly yield additional information to add to the growing knowledge base on hydrogen bonding in proteins.

Materials and methods

Mutagenesis and protein purification

Mutation at residue 31 of HPr was performed using the wild-type gene carried in pUC13 as have previously been described (Anderson et al., 1991; Sharma et al., 1991) using the general procedures of Zoller and Smith (1984), as modified by Kunkel (1985). The primer used was 5′-AGTAATTTCCGGAGTGAAG CC-3′. Both HPr and S31A were overexpressed in transformed *E. coli* strain TP2811 F′,*xylargH1lacX74aroBlevAΔ(ptsHptsIcrr), KmR* (Levy et al., 1990) and purified by the protocol previously described (Anderson et al., 1991). Yields were approximately 200 mg/20 g wet weight cells. Protein that was uniformly labeled with ^{15}N was generated as previously described (Hammen et al., 1991). Yields were approximately 60 mg/10 g wet weight cells. All preparations were judged to be homogeneous by isoelectric focusing.

Activity measurements

Phosphohydrolysis, protein determination, and assays for enzyme I and the mannitol-, mannose-, and *N*-acetylglucosamine-specific enzymes II were performed as previously described (Anderson et al., 1991).

Protein stability

CD at 222 nm was used to monitor the equilibrium unfolding data using an Aviv 62DS spectropolarimeter equipped with a temperature control and stirring unit. The urea-denaturation curves at 30 °C were performed with urea solutions that were prepared fresh daily in buffered solutions containing 50 mM potassium phosphate at pH 7.0. The concentration of the urea stock solution was determined by refractive index measurements (Pace, 1986). The details of the method used for the urea denaturation curves are described by Scholtz (1995).

The urea denaturation curves were analyzed by assuming a two-state unfolding reaction, and the pre- and post-transition regions of the curves were treated as linear baseline effects on the CD signal with molar urea concentration. The nonlinear least-squares fitting employed the algorithm that is based on the method described by Johnson and Frasier (1985) and implemented for the Macintosh computer (Brenstein, 1991). The anal-

ysis of a single denaturation curve can be used to find the values for the best-fit parameters and their confidence intervals (Santoro & Bolen, 1988). From repeated measurements on these and other proteins, the uncertainty on the $\Delta\Delta G$ value is estimated to be 0.15 kcal mol^{-1}, even though the standard error from the analysis of a single urea denaturation curve is much smaller. We feel that the uncertainty based on repeated measurements gives a more reliable estimate of the error on $\Delta\Delta G$ values.

NMR spectroscopy

Samples were prepared by dialyzing purified protein against buffer containing 5 mM potassium phosphate and 0.01 mM EDTA at pH 6.5. After dialysis, the solutions were lyophilized and dissolved in 90% deionized H_2O and 10% D_2O. The final solutions were ca. 4 mM in protein, 50 mM in potassium phosphate, and 0.1 mM in EDTA. NMR spectra were acquired on a modified Bruker AM-500 spectrometer. Unless noted otherwise, all spectra were recorded at pH 6.5 and 30 °C. Two-dimensional spectra were obtained in the pure-phase absorption mode using time-proportional phase incrementation (Marion & Wüthrich, 1983). The water signal was suppressed by saturation between acquisitions and during NOESY mixing times. Data were processed using FELIX 1.0 (Hare Research, Woodinville, Washington) on a Silicon Graphics 4D-35 workstation. Homonuclear 2D data sets were typically 600 × 2K complex points, processed with sine-bell weighting functions skewed toward $t = 0$ and shifted by $\pi/3$ in both dimensions. During processing, they were zero-filled to produce 2K × 2K matrices. Baseplane corrections were made using the method of Dietrich et al. (1991). Both ^1H and ^{15}N chemical shifts were referenced as previously described (Hammen et al., 1991). ^1H chemical shift assignments for S31A were made with the use of DQF-COSY spectra (Muller et al., 1986) and clean-TOCSY spectra using 70 ms for the mixing sequence (Griesinger et al., 1988). Homonuclear NOESY spectra were collected with a mixing time of 100 ms. ^{15}N chemical shifts, values of $^3J_{NH\alpha}$, and NH exchange rates were obtained using 2D ^{15}N-^1H spectroscopy as previously described (Hammen et al., 1991). The smallest measurable splitting in the (^{15}N-^1H) HMQC-J spectra of S31A was 4 Hz, whereas that in the HPr data was 2.5 Hz (Hammen et al., 1991). Exchange rates for slowly exchanging amide protons were determined by fitting the logarithm of signal intensity (measured by volumes of (^{15}N-^1H) HMQC peaks) as a function of time following dissolution of the sample in D_2O at 30 °C by a linear least-squares analysis. Spectra were collected continuously, with each spectrum requiring 15 min to collect. Correlation coefficients for the fits were all greater than 0.95. Exchange behavior of the more rapidly exchanging amide protons was measured by methods that have been previously described, using an average T_1 value of 0.3 s (Spera et al., 1991; Rajagopal et al., 1994). To separate chemical exchange effects from those that result from magnetization transfer, experiments were carried out at three pH values: pH 6.5, 7.2, and 8.1. (^{15}N,^1H) HNHB experiments were carried out using the pulse sequence and adjustable parameters described in Figure 1A of Archer et al. (1991).

Structural analysis

Structures were visualized and analyzed using INSIGHT (Biosym, Inc.). Steric clashes were viewed using the BUMP algorithm with an overlap of 0.15 Å while interactively rotating Asp 69 about χ_1. Hydrogen bond characteristics were obtained using the program HBPLUS version 3.15 (McDonald & Thornton, 1994).

Acknowledgments

We thank Dr. Ponni Rajagopal for collecting 2D TOCSY spectra and for useful discussions and Dr. Bryan Jones for preparing Figure 5. We also thank the anonymous reviewer who suggested that we evaluate the conformational changes in entropy of our system. This work was supported by NIH grant RO1 DK13587 (R.E.K.), Robert A. Welch Foundation grant A-1281 (J.M.S.), and MRC operating grant MT6147 (E.B.W.).

References

Anderson JW, Bhanot P, Georges F, Klevit RE, Waygood EB. 1991. Involvement of the carboxy-terminal residue in the active site of the histidine-containing protein, HPr, of the phosphoenolpyruvate:sugar phosphotransferase system of *Escherichia coli*. *Biochemistry 30*:9601–9607.

Archer SJ, Ikura M, Torchia DA, Bax A. 1991. An alternative 3D NMR technique for correlating backbone ^{15}N with side chain ^1H resonances in larger proteins. *J Magn Reson 95*:636–641.

Brenstein RJ. 1991. *NonLin for Macintosh*. Carbondale, Illinois: Robelko Software.

Dietrich W, Rudel CH, Neumann M. 1991. Fast and precise automatic baseline correction of one- and two-dimensional NMR spectra. *J Magn Reson 91*:1–11.

Driscoll PC, Gronenborn AM, Wingfield PT, Clore GM. 1990. Determination of the secondary structure and molecular topology of interleukin-1 by use of two- and three-dimensional heteronuclear ^{15}N-^1H NMR spectroscopy. *Biochemistry 29*:4668–4682.

Driscoll PC, Hill HA, Redfield C. 1987. ^1H-NMR sequential assignments and cation-binding studies of spinach plastocyanin. *Eur J Biochem 170*: 279–292.

Fauchère JL, Pliska V. 1983. Hydrophobic parameters π of amino acid side-chains from the partitioning of *N*-acetyl-amino-acid amides. *Eur J Med Chem-Chim Ther 18*:369–375.

Feng Y, Roder H, Englander SW, Wand AJ, Di Stefano DL. 1989. Proton resonance assignments of horse ferricytochrome *c*. *Biochemistry 28*: 195–203.

Gao Y, Boyd J, Williams RJ, Pielak GJ. 1990. Assignment of proton resonances, identification of secondary structural elements, and analysis of backbone chemical shifts for the C102T variant of yeast iso-1-cytochrome *c* and horse cytochrome *c*. *Biochemistry 29*:6994–7003.

Griesinger C, Otting G, Wüthrich K, Ernst RR. 1988. Clean TOCSY for ^1H spin system identification in macromolecules. *J Am Chem Soc 110*: 7870–7872.

Hammen PK, Waygood EB, Klevit RE. 1991. Reexamination of the secondary and tertiary structure of histidine-containing protein from *Escherichia coli* by homonuclear and heteronuclear NMR spectroscopy. *Biochemistry 30*:11842–11850.

Herzberg O, Klevit RE. 1994. Unraveling a bacterial hexose transport pathway. *Curr Opin Struct Biol 4*:814–822.

Herzberg O, Reddy P, Sutrina S, Saier MH Jr, Reizer J, Kapafia G. 1992. Structure of the histidine-containing phosphocarrier protein HPr from *Bacillus subtilis* at 2.0 Å-resolution. *Proc Natl Acad Sci USA 89*:2499–2503.

Jia Z, Quail JW, Waygood EB, Delbaere LTJ. 1993a. The 2.0-Å resolution structure of *Escherichia coli* histidine-containing phosphocarrier protein HPr. *J Biol Chem 268*:22490–22501.

Jia Z, Vandonselaar M, Quail JW, Delbaere LTJ. 1993b. Active-centre torsion-angle strain revealed in 1.6 Å-resolution structure of histidine-containing phosphocarrier protein. *Nature (Lond) 361*:94–97.

Johnson MJ, Frasier SG. 1985. Nonlinear least-squares analysis. *Methods Enzymol 117*:301–342.

Kalbitzer HR, Hengstenberg W. 1993. The solution structure of the histidine-containing protein (HPr) from *Staphylococcus aureus* as determined by two-dimensional ^1H-NMR spectroscopy. *Eur J Biochem 216*:205–214.

Kalbitzer HR, Neidig KP, Hengstenberg W. 1991. Two-dimensional ^1H NMR studies on HPr protein from *Staphylococcus aureus*: Complete sequential assignments and secondary structure. *Biochemistry 30*:11186–11192.

Klevit RE, Waygood EB. 1986. Two-dimensional ^1H NMR studies of

histidine-containing protein from *Escherichia coli*. 3. Secondary and tertiary structure as determined by NMR. *Biochemistry 25*:7774–7781.

Kunkel TA. 1985. Rapid and efficient site-specific mutagenesis without phenotypic selection. *Proc Natl Acad Sci USA 82*:488–492.

Levy S, Zeng GQ, Danchin A. 1990. Cyclic AMP synthesis in *Escherichia coli* strains bearing known deletions in the pts phosphotransferase operon. *Gene (Amst) 86*:27–33.

Marion D, Wüthrich K. 1983. Application of phase-sensitive two-dimensional correlated spectroscopy (COSY) for measurements of spin–spin coupling constants in proteins. *Biochem Biophys Res Commun 113*:967–974.

McDonald IK, Thornton JM. 1994. Satisfying hydrogen bonding potential in proteins. *J Mol Biol 238*:777–793.

Muller N, Ernst RR, Wüthrich K. 1986. Multiple-quantum filtered two-dimensional correlated NMR spectroscopy of proteins. *J Am Chem Soc 108*:6482–6492.

Pace CN. 1986. Determination and analysis of urea and guanidine hydrochloride denaturation curves. *Methods Enzymol 131*:266–280.

Pickett SD, Sternberg MJE. 1993. Empirical scale of side-chain conformational entropy in protein folding. *J Mol Biol 231*:825–839.

Rajagopal P, Waygood EB, Klevit RE. 1994. Structural consequences of histidine phosphorylation: NMR characterization of the phosphohistidine form of histidine-containing protein from *Bacillus subtilis* and *Escherichia coli*. *Biochemistry 33*:15271–15282.

Santoro MM, Bolen DW. 1988. Unfolding free energy changes determined by the linear extrapolation method. 1. Unfolding of phenylmethanesulfonyl α-chymotrypsin using different denaturants. *Biochemistry 27*:8063–8068.

Scholtz JM. 1995. Conformational stability of HPr: The histidine-containing phosphocarrier protein from *Bacillus subtilis*. *Protein Sci 4*:35–43.

Sharma S, Georges F, Delbaere LTJ, Lee JS, Klevit RE, Waygood EB. 1991. Epitope mapping by mutagenesis distinguishes between the two structures of the histidine-containing protein HPr. *Proc Natl Acad Sci USA 88*:4877–4881.

Sharp KA, Nicholls A, Friedman R, Honig B. 1991. Extracting hydrophobic free energies from experimental data: Relationship to protein folding and theoretical methods. *Biochemistry 30*:9686–9697.

Shirley BA, Stanssens P, Hahn U, Pace CN. 1992. Contribution of hydrogen bonding to the conformational stability of ribonuclease T1. *Biochemistry 31*:725–732.

Spera S, Ikura M, Bax A. 1991. Measurement of the exchange rates of rapidly exchanging amide protons: Application to the study of calmodulin and its complex with a myosin light chain kinase fragment. *J Biomol NMR 1*:155–165.

van Nuland NAJ, Grotzinger J, Dijkstra K, Scheek RM, Robillard GT. 1992. Determination of the three-dimensional solution structure of the histidine-containing phosphocarrier protein HPr from *Escherichia coli* using multidimensional NMR spectroscopy. *Eur J Biochem 210*:881–891.

van Nuland NAJ, Hangyi IW, van Schaik RC, Berendsen HJC, van Gunsteren WF, Scheek RM, Robillard GT. 1994. The high-resolution structure of the histidine-containing phosphocarrier protein HPr from *Escherichia coli* determined by restrained molecular dynamics from nuclear magnetic resonance nuclear Overhauser effect data. *J Mol Biol 237*:544–559.

Wittekind M, Rajagopal P, Branchini BR, Reizer J, Saier MH Jr, Klevit RE. 1992. Solution structure of the histidine-containing protein from *Bacillis subtilis*. *Protein Sci 1*:1363–1376.

Zoller MJ, Smith M. 1984. Oligonucleotide-directed mutagenesis: A simple method using two oligonucleotide primers and a single-stranded DNA template. *DNA (NY) 3*:479–488.